



# Effect of swelling on spatial inhomogeneity in poly(acrylamide) gels formed at various monomer concentrations

Mine Yener Kizilay, Oguz Okay\*

*Department of Chemistry, Istanbul Technical University, 80626 Maslak, Istanbul, Turkey*

Received 5 October 2003; received in revised form 20 January 2004; accepted 26 January 2004

## Abstract

The effect of swelling on the spatial inhomogeneity in poly(acrylamide) (PAAm) gels has been investigated with the static light scattering measurements. Four sets of gels were prepared using *N,N'*-methylenebis(acrylamide) (BAAm) as a crosslinker at various initial monomer concentrations. The crosslinker ratio  $X$  (the mole ratio of BAAm to the monomer acrylamide) was fixed at 1/50, 1/61.5, 1/66, and 1/100 in each set of gels. The gels, both at the state of preparation and at the equilibrium swollen state in water, exhibit a maximum degree of spatial gel inhomogeneity at a critical monomer concentration ( $\nu_{2,cr}^0$ ).  $\nu_{2,cr}^0$  shifts toward smaller concentrations as  $X$  is decreased or, as the gel swells beyond its swelling degree after preparation. Swelling enhances the extent of spatial inhomogeneity in PAAm gels and, this enhancement mainly occurs at low crosslinker ratios. The theoretical prediction of the Panyukov–Rabin theory was found to be in qualitative agreement with the experimental findings. It was also shown that three different effects, namely crosslinker, concentration, and swelling effects determine the extent of inhomogeneities in gels formed at various monomer concentrations.

© 2004 Elsevier Ltd. All rights reserved.

*Keywords:* Poly(acrylamide) gels; Inhomogeneity; Static light scattering

## 1. Introduction

In contrast to ideal gels with a homogeneous distribution of crosslinks, real gels always exhibit an inhomogeneous crosslink density distribution, known as the spatial gel inhomogeneity [1,2]. The inhomogeneities present in gels are of considerable interest and importance in attempts to characterize such materials physically. From the practical point of view, spatial inhomogeneity is undesirable because it dramatically reduces the optical clarity and strength of gels, which are properties closely connected with many industrial applications such as contact lenses, super absorbents, etc.

Since the spatial gel inhomogeneity necessarily produces local concentration fluctuations in gels, scattering methods have been used to investigate the inhomogeneities [3–9]. The gel inhomogeneity can be manifested by comparing the scattering intensities from the gel and from a semi-dilute solution of the same polymer at the same concentration. The

excess scattering over the scattering from polymer solution is related to the degree of the inhomogeneities in gels. In general, the gel inhomogeneity increases with the gel crosslink density due to the simultaneous increase of the extent of network imperfections producing regions more or less rich in crosslinks [10–15]. Degree of swelling of gels subjected to scattering measurements also affects the scattering intensities. Bueche reported in 1970 the enhancement of scattering intensity associated with the swelling of polymer networks [16]. Later, various types of gels have been investigated at different swelling stages [2,17–19]. The results show that the scattering intensity at low scattering vectors is enhanced as the swelling degree is increased. This behavior was interpreted as the enhancement of the difference of polymer concentration between the more and the less crosslinked regions.

The initial monomer concentration used in the gel preparation significantly affects the network structure, and, in turn, affects the gel properties [20–22]. In our previous paper, we discussed the monomer concentration dependence of the spatial inhomogeneities in poly(acrylamide) (PAAm) gels formed at a fixed crosslinker ratio [23]. Contrary to the expectation that the gel inhomogeneity

\* Corresponding author. Tel.: +90-212-2853156; fax: +90-212-2856386.

*E-mail address:* [okayo@itu.edu.tr](mailto:okayo@itu.edu.tr) (O. Okay).

should always decrease with the monomer concentration, we found a critical monomer concentration, where the degree of the gel inhomogeneity attains a maximum value. This phenomenon was explained as a result of two opposite effects of the monomer concentration on the gel inhomogeneity [23]. As the monomer concentration is increased, the effective density of crosslinks also increases, so that the spatial inhomogeneity becomes larger. Opposing this, increasing monomer concentration, i.e. decreasing the degree of swelling of gels after preparation reduces progressively the concentration difference between densely and loosely crosslinked regions of gel, so that the apparent inhomogeneity decreases. The interplay of these two opposite effects seems to determine the inhomogeneity in PAAm gels and results in the appearance of a maximum gel inhomogeneity at a critical monomer concentration.

The observations reported above were made on PAAm gels at a gel state just after their preparation. In the present work, we have investigated the effect of swelling on the spatial inhomogeneity in PAAm gels formed at various monomer concentrations. The questions whether the maximum observed in the spatial gel inhomogeneity vs. monomer concentration dependence still exists for the equilibrium swollen PAAm gels and how this dependence varies depending on the degree of swelling were the subject of the present study. We prepared four sets of PAAm gels by free-radical crosslinking copolymerization of acrylamide (AAm) and N,N'-methylenebis(acrylamide) (BAAm) monomers at various initial monomer concentration. The crosslinker ratio  $X$ , that is the mole ratio of the crosslinker BAAm to the monomer AAm was fixed at 1/50, 1/61.5, 1/66, and 1/100 in each set of gels. For each gel sample, the spatial inhomogeneities were characterized by static light scattering measurements at two gel states; (a) just after the preparation state, and (b) equilibrium swollen state in water. A semi-dilute PAAm solution of the same concentration as the equivalent gel served as a reference in the understanding of the inhomogeneities in gels. The excess scattering from the gels is taken as a measure of their inhomogeneity. In addition, swelling and elasticity measurements have as well been carried out to find the effective crosslink densities of gels formed at various concentrations. The experimental results were compared with the predictions of the statistical theory proposed by Panyukov and Rabin [24].

## 2. Experimental section

### 2.1. Synthesis of hydrogels

Acrylamide (AAm, Merck), N,N'-methylenebis(acrylamide) (BAAm, Merck), ammonium persulfate (APS, Merck), and N,N,N',N'-tetramethylethylenediamine (TEMED) were used as received. PAAm gels were prepared by free-radical crosslinking copolymerization of AAm and BAAm in an aqueous solution at 24 °C in the presence of

2.63 mM APS initiator and 0.375 v/v% TEMED accelerator. The gels were prepared as four sets; in each set, the initial molar concentration of the monomers, denoted by  $C_0$ , was varied between 0.36 and 2.09 M while the crosslinker ratio  $X$  (the mole ratio of BAAm to AAm) was fixed at 1/50, 1/61.5, 1/66, or 1/100. The reaction time was one day. Details about the gel synthesis have been reported elsewhere [25].

### 2.2. PAAm network concentration at the stage of gel preparation

The degree of dilution of the networks after their preparation was denoted by  $\nu_2^0$ , the volume fraction of crosslinked polymer after the gel preparation. In order to determine  $\nu_2^0$ , PAAm hydrogels after preparation were extracted in water over a period of at least one month. The hydrogels after extraction were first deswollen in water–acetone mixtures and then dried at 90 °C under vacuum to constant weight. Details about the extraction procedure were described previously [26]. Measurements showed that the experimental value of  $\nu_2^0$  is close to its theoretical value  $\nu_2^0 = 10^{-3}C_0V_r$ , where  $V_r$  is the molar volume of PAAm repeat units (52.6 ml/mol, calculated using the PAAm density  $\rho = 1.35$  g/ml). This indicates that, under the reaction conditions, the monomer conversions and the gel fractions are complete.

### 2.3. Swelling measurements in water

The hydrogels in the form of rods of 4 mm in diameter were cut into samples of about 10 mm length. Then, each sample was placed in an excess of water at  $24 \pm 0.5$  °C. In order to reach swelling equilibrium, the hydrogels were immersed in water for at least two weeks replacing the water every other day. The swelling equilibrium was tested by measuring the diameter of the gel samples. To achieve good precision, three measurements were carried out on samples of different length taken from the same gel. The normalized volume of the equilibrium swollen hydrogels  $V_{eq}$  (volume of equilibrium swollen gel/volume of the gel just after preparation) was determined by measuring the diameter of the hydrogel samples by a calibrated digital compass (Mitutoyo Digimatic Caliper, Series 500, resolution: 0.01 mm).  $V_{eq}$  was calculated as

$$V_{eq} = (D/D_0)^3 \quad (1)$$

where  $D$  and  $D_0$  are the diameter of hydrogels after equilibrium swelling in water and after synthesis, respectively. The volume fraction of crosslinked polymer in the equilibrium swollen gel  $\nu_{2,eq}$  was calculated as

$$\nu_{2,eq} = \frac{\nu_2^0}{V_{eq}} \quad (2)$$

## 2.4. Mechanical measurements

Uniaxial compression measurements were performed on gels just after their preparation. All the mechanical measurements were conducted in a thermostated room of  $24 \pm 0.5$  °C. The stress–strain isotherms were measured by using an apparatus previously described [27]. The elastic modulus  $G_0$  was determined from the slope of linear dependence  $f = G_0(\alpha - \alpha^{-2})$ , where  $f$  is the force acting per unit cross-sectional area of the undeformed gel specimen, and  $\alpha$  is the deformation ratio (deformed length/initial length). For a network of Gaussian chains, the elastic modulus at the state of gel preparation  $G_0$  is related to the effective crosslink density  $\nu_e$  by [28,29]:

$$G_0 = A\nu_e RT\nu_2^0 \quad (3)$$

where the front factor  $A$  equals to 1 for an affine network and  $1-2/\phi$  for a phantom network, where  $\phi$  is the functionality of the crosslinks,  $R$  and  $T$  are in their usual meanings. Since the gels prepared in this study were highly swollen, we used phantom network model ( $\phi = 4$ ) to calculate the effective crosslink densities of PAAm gels.

## 2.5. Light scattering experiments

For the light scattering measurements, the crosslinking polymerizations were carried out in the light scattering vials. All glassware was kept dustfree by rinsing in hot acetone prior using. The solutions were filtered through membrane filters (pore size, 0.2  $\mu\text{m}$ ) directly into the vials. This process was carried out in a dustfree glovebox. All the gels subjected to light scattering measurements were clear and appeared homogeneous to the eye.

The light scattering measurements were carried out at 24 °C using a commercial multi-angle light scattering DAWN EOS (Wyatt Technologies Corporation) equipped with a vertically polarized 30 mW Gallium–arsenide laser operating at  $\lambda = 690$  nm and 18 simultaneously detected scattering angles. The scattered light intensities were recorded from 51.5 to 142.5° which correspond to the scattering vector  $q$  range  $1.1 \times 10^{-3}$ – $2.3 \times 10^{-3}$   $\text{\AA}^{-1}$ , where  $q = (4\pi n/\lambda)\sin(\theta/2)$ ,  $\theta$  the scattering angle,  $\lambda$  the wavelength of the incident light in vacuum,  $n$  the refractive index of the medium. The light scattering system was calibrated against a toluene standard (Rayleigh ratio at 690 nm =  $9.7801 \times 10^{-6}$   $\text{cm}^{-1}$ , DAWN EOS software). To obtain the ensemble averaged light scattering intensity of gels, eight cycles of measurements with a small rotation of the vial between each cycle were averaged.

The measurements were carried out on gels both at the state of gel preparation and at the equilibrium swollen state in water. For the calculation of excess scattering from gels, all the crosslinking polymerizations were repeated under the same experimental conditions except that the crosslinker BAAM was not used. To calculate the excess scattering

from swollen gels, polymer solutions were diluted to obtain solutions at the same polymer concentration as the swollen gels. Necessary dilution degrees for PAAm solutions were calculated from the equilibrium swelling ratios  $V_{\text{eq}}$  using the equation:

$$V_{\text{sol}} = V_{0,\text{sol}}V_{\text{eq}} \quad (4)$$

where  $V_{0,\text{sol}}$  and  $V_{\text{sol}}$  are the solution volumes before and after dilution with water.

As is well known, the use of TEMED as the accelerator during the gelation process leads to the formation of charged groups in the aged PAAm gels. The number of charged groups increases, and therefore, the Rayleigh ratio  $R(q)$  decreases with increasing time of aging of PAAm gels in the polymerization reactor [14]. However, our previous work shows that  $R(q)$  does not change as long as the aging time is less than 5 days [14]. Therefore, for the present gels with one day aging, the effect of hydrolysis on spatial inhomogeneity can be neglected.

## 3. Results

Four sets of PAAm gels were prepared, each at a fixed crosslinker ratio  $X$  but at various polymer network concentrations  $\nu_2^0$ . Fig. 1 shows the volume fraction of crosslinked polymer in the equilibrium swollen gel  $\nu_{2,\text{eq}}$  and the effective crosslink density  $\nu_e$  of the hydrogels plotted as a function of  $\nu_2^0$ . Data for  $X = 1/61.5$ , 1/66, and 1/100 were taken from the literature [23], while those for  $X = 1/50$  are results of new measurements. The solid curves are polynomial best fits to each set of the experimental data. The coefficients of the fit equations compiled in Table 1 will be used in the following section for the analysis of the light scattering results. As expected,  $\nu_{2,\text{eq}}$  and  $\nu_e$  are increasing functions of both the polymer network concentration  $\nu_2^0$  and the crosslinker ratio  $X$ , that is, the higher the initial monomer concentration, or, the higher the crosslinker ratio, the larger the effective crosslink density of the hydrogels and the smaller their swelling capacity.

Light scattering measurements were carried out on gel samples just after their preparation and after equilibrium swelling in water. Fig. 2 shows the Rayleigh ratio  $R(q)$  vs.

Table 1

The coefficients of the fit equations  $\nu_e(\text{or } \nu_{2,\text{eq}}) = a + b\nu_2^0 + c(\nu_2^0)^2$  showing the monomer concentration dependence of the effective crosslink density ( $\nu_e$  in  $\text{mol}/\text{m}^3$ ) and the polymer volume fraction in the equilibrium swollen gel ( $\nu_{2,\text{eq}}$ )

$X$	$\nu_e =$			$\nu_{2,\text{eq}} =$		
	$a$	$b$	$c$	$a$	$b$	$c$
1/50	−129	5215	−13057	−0.01548	1.13682	−1.23848
1/61.5	−64	3064	−691	−0.01112	0.86854	1.02450
1/66	−61	2509	6453	−0.01525	1.05653	−2.49385
1/100	−42	1888	2540	−0.01476	0.83390	0.23720

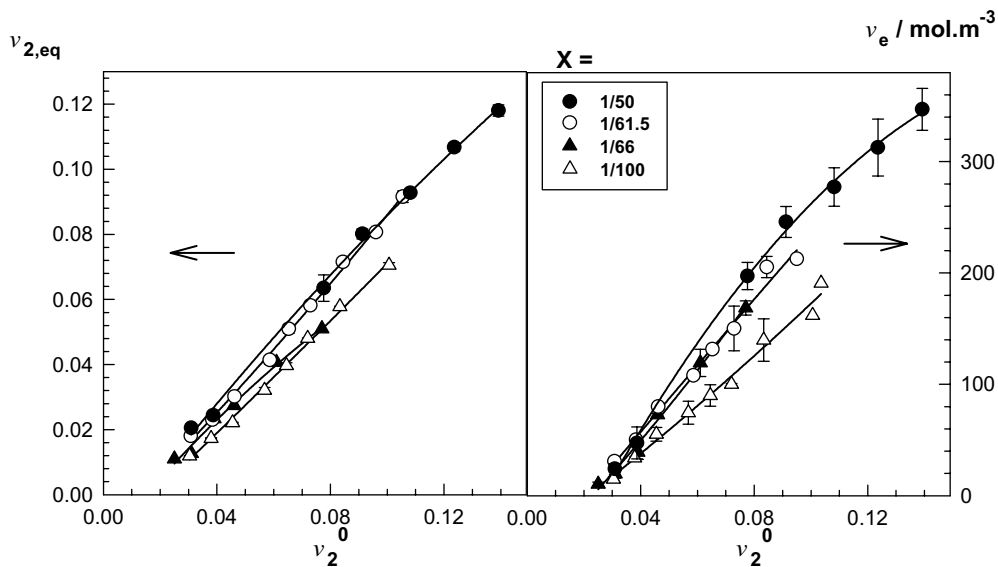


Fig. 1. The volume fraction of crosslinked polymer in the equilibrium swollen gel  $\nu_{2,eq}$  and the effective crosslink density  $\nu_e$  of the hydrogels shown as a function of the polymer network concentration  $\nu_2^0$ . The crosslinker ratios  $X$  of the hydrogels are indicated in the Figure. Data for  $X = 1/66, 1/61.5$  and  $1/100$  were taken from Ref. [23]. The curves are polynomial best fits to each set of data with coefficients listed in Table 1.

the scattering vector  $q$  plots for PAAM gels swollen to equilibrium in water and for the corresponding linear PAAM solutions of the same concentration. The crosslinker ratio  $X$  of gels was fixed at  $1/61.5$ . Light scattering intensity from solutions  $R_{sol}(q)$  does not change much with the polymer concentration  $\nu_2^0$  and with the scattering vector  $q$  (Fig. 2A). However, a closer examination of the solution data shown as inset to Fig. 2A indicates a slight decrease of the scattered light intensity from polymer solution with increasing concentration. Light scattering intensity from gels  $R_{gel}(q)$  first increases with  $\nu_2^0$  up to a critical value ( $\nu_{2,cr}^0$ ) but then decreases again (Figs. 2B and C). Similar results such as those in Fig. 2 were obtained for other sets of gels both at the state of preparation and at their swollen states.

To compare the scattering intensities of various gels at different states, we will focus on the scattering intensity  $R_q$  measured at a fixed scattering vector  $q = 1 \times 10^{-3} \text{ \AA}^{-1}$ .

Fig. 3 shows  $R_{sol,q}$  (triangles) and  $R_{gel,q}$  (circles) plotted as a function of  $\nu_2^0$  for gels with  $X = 1/66$ . The filled and open symbols represent results of measurements on gels (or solutions) after preparation and after equilibrium swelling in water (or after dilution with water), respectively.  $R_{sol,q}$  slightly decreases on dilution of PAAM solutions, while  $R_{gel,q}$  significantly increases as the gel swells beyond its swelling degree after preparation. Moreover, PAAM gels at both states exhibit a maximum scattering intensity  $R_{gel,q}$  at a critical polymer network concentration, denoted by  $\nu_{2,cr}^0$ . Other sets of gels gave similar results.

Excess scattering intensities  $R_{ex,q}$  were calculated from the scattering intensities of gels and solutions as follows:

$$R_{ex,q} = R_{gel,q} - R_{sol,q} \tag{5}$$

Since the thermal fluctuations are eliminated in Eq. (5), excess scattering  $R_{ex,q}$  is a measure of the degree of spatial

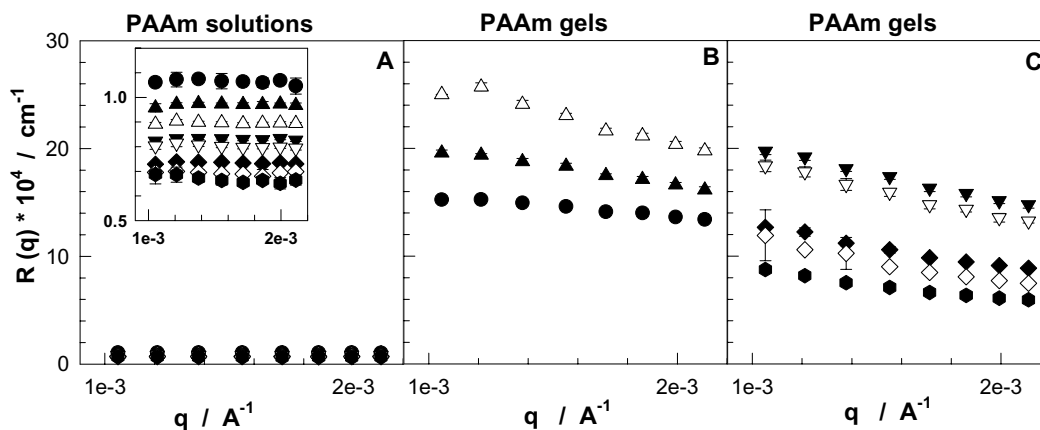


Fig. 2. Rayleigh ratio  $R(q)$  versus scattering vector  $q$  plots for the equilibrium swollen PAAM gels (B and C) and for the corresponding linear PAAM solutions (A).  $X = 1/61.5, \nu_2^0 = 0.030$  (●),  $0.046$  (▲),  $0.058$  (△),  $0.065$  (▼),  $0.073$  (▽),  $0.084$  (◆),  $0.096$  (◇), and  $0.103$  (●).

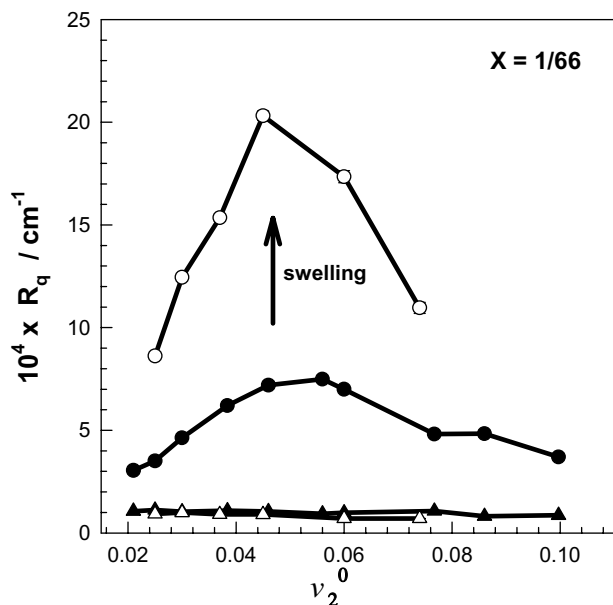


Fig. 3. Scattering light intensities from gels  $R_{gel,q}$  (circles) and from PAAM solutions  $R_{sol,q}$  (triangles), both measured at  $q = 1 \times 10^{-3} \text{ \AA}^{-1}$  shown as a function of  $\nu_2^0$ . The filled and open symbols represent results of measurements on gels (or on solutions) after preparation and after equilibrium swelling in water (or after dilution with water), respectively. The crosslinker ratio  $X = 1/66$ .

inhomogeneities in gels. Figs. 4A–D show  $R_{ex,q}$  of gels after preparation (filled symbols) and after equilibrium swelling in water (open symbols) plotted against the concentration  $\nu_2^0$ . The crosslinker ratios for each set of gels are indicated in the Figures. Note that the gels with the highest crosslinker ratio ( $X = 1/50$ ) became opaque in the range of  $\nu_2^0$  between 0.045 and 0.070, represented by the dark area in Fig. 4A. The appearance of opacity indicates that these gels have phase-separated domains in a spatial scale of submicrometer to micrometer. Thus, at this relatively high crosslinker ratio, an insolubility gap exists in this range of  $\nu_2^0$ , outside which  $R_{ex,q}$  decreases, i.e. the gel becomes increasingly homogeneous as the distance from the critical range is increased.

A general trend seen in Fig. 4 is the enhancement of the degree of spatial inhomogeneity during swelling of PAAM gels with respect to the state of preparation. This enhancement mainly occurs at low crosslinker ratios  $X$ ; a 2–3 fold increase in  $R_{ex,q}$  was observed during the swelling process of the hydrogels with  $X = 1/66$  and  $1/100$ . For the highly crosslinked gels,  $R_{ex,q}$  is rather constant in the vicinity of  $\nu_{2,cr}^0$  irrespective of the gel state, while it slightly increases at low or high concentration tails of  $\nu_{2,cr}^0$  during the gel swelling. Another point shown in Fig. 4 is that  $\nu_{2,cr}^0$  shifts toward lower polymer concentrations as the crosslinker ratio  $X$  is decreased or, as the gel swells beyond its swelling degree after preparation. In Fig. 5, the ratio  $R_{ex,q}/R_{gel,q}$ , representing the contribution of the spatial inhomogeneities to the scattering light intensity from PAAM gels is plotted against  $\nu_2^0$  for gels after preparation (A) and for the equilibrium swollen gels (B). It is seen that the spatial

inhomogeneity contributes 80–100% of the scattered light intensity from swollen gels, which is much larger than that measured from gels at the state of their preparation. Moreover, the maxima in  $R_{ex,q}/R_{gel,q}$  vs.  $\nu_2^0$  plots become almost invisible in swollen gels due to the large increase in the excess scattering intensities at low and high polymer concentrations.

#### 4. Discussion

To interpret the light scattering results from gels, several Lorentzian and Gaussian scattering functions have been proposed empirically [16,30–37]. For example, the excess scattering  $R_{ex}(q)$  was given by the Debye–Bueche (DB) function as [16,30–32]:

$$R_{ex}(q) = \frac{4\pi K \xi^3 \langle \eta^2 \rangle}{(1 + q^2 \xi^2)^2} \quad (6)$$

where  $K$  being the optical constant,  $K = 8\pi^2 n^2 \lambda^{-4}$ ,  $\xi$  is the correlation length of the scatterers, and  $\langle \eta^2 \rangle$  is the mean square fluctuation of the refractive index. Note that the correlation length  $\xi$  of DB theory is a characteristic length scale in the gel and, it is a measure of the spatial extent of the fluctuations. According to Eq. (6), the slope and the intercept of  $R_{ex}(q)^{-1/2}$  vs  $q^2$  plot (DB plot) give  $\xi$  and  $\langle \eta^2 \rangle$  of a gel sample [14]. Calculated values of  $\xi$  and  $\langle \eta^2 \rangle$  from DB analysis are shown in Fig. 6 plotted as a function of  $\nu_2^0$ . Open symbols are for swollen gels while filled symbols are for gels after preparation. The correlation length of the scatterers  $\xi$  and the mean square fluctuations  $\langle \eta^2 \rangle$  are in the range of 6–27 nm and  $10^{-7}$ – $10^{-5}$ , respectively.  $\xi$  increases as the polymer concentration  $\nu_2^0$  increases, while  $\langle \eta^2 \rangle$  vs.  $\nu_2^0$  dependence exhibits a maximum between  $\nu_2^0 = 0.03$  and  $0.04$  for each set of gels. Moreover, a general trend is that both  $\xi$  and  $\langle \eta^2 \rangle$  slightly increases during swelling of PAAM gels.

Although DB theory can successfully be used to derive the characteristic parameters of inhomogeneous gels, it does not give a correlation between the gel synthesis parameters and the degree of the gel inhomogeneity. Recently, Panyukov and Rabin proposed a statistical theory for describing the structural factor for gels [24]. The Panyukov–Rabin (PR) theory assumes that the gel is prepared by instantaneous crosslinking of semi-dilute polymer solutions. The advantage of PR theory is that there is no assumption about the functional dependence of excess scattering on the scattering vector, as in the DB theory. This theory also predicts the correlations between the synthesis parameters of gels and their scattering properties. The PR theory takes into account the effect of the network structure at preparation on the structure factor  $S(q)$  under condition of measurements. The structure factor of this theory consists of two contributions, one from the thermal fluctuations  $G(q)$  and the other from the static inhomogeneities  $C(q)$ .

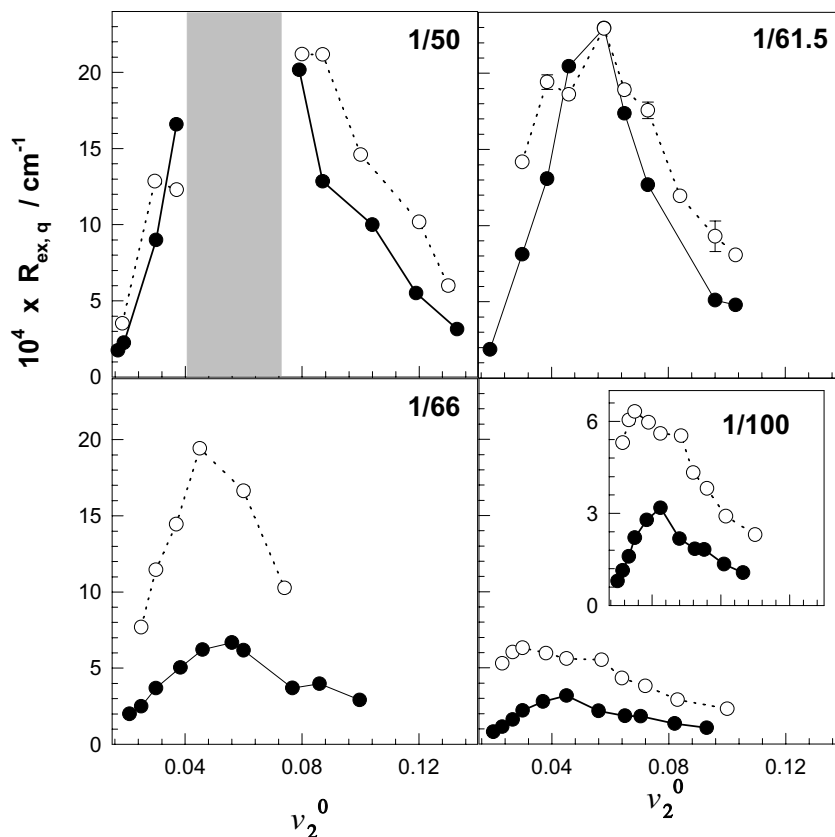


Fig. 4. Excess scattering intensities  $R_{\text{ex},q}$  at  $q = 1 \times 10^{-3} \text{ \AA}^{-1}$  shown as a function of  $\nu_2^0$ . The filled and open symbols represent data of gels at the state of their preparation and at the equilibrium swollen state in water, respectively. The crosslinker ratios  $X$  are indicated in the figures.

Theoretical prediction of the PR theory requires the network parameters at the state of the gel preparation as well as at the state of the measurements. According to the PR theory, these structure factors are given by the following equations:

$$S(q) = G(q) + C(q) \quad (7)$$

$$G(q) = \frac{a^{-3} \nu_2 N g(q)}{1 + wg(q)} \quad (8)$$

$$C(q) = \frac{a^{-3} \nu_2 N}{(1 + wg(q))^2 (1 + Q^2)^2} \times \left( 6 + \frac{9}{w_0 - 1 + 0.5Q^2(\nu_2^0/\nu_2)^{2/3}} \right) \quad (9)$$

where  $a$  is the segment length,  $\nu_2$  is the volume fraction of crosslinked polymer in the gel at the measurement,  $N$  is the number of segments between two successive crosslinks, and  $g(q)$  is the thermal correlator in the absence of the excluded volume effect,

$$g(q) = \frac{1}{0.5Q^2 + (4Q^2)^{-1} + 1} + \frac{2(\nu_2/\nu_2^0)^{2/3}}{(1 + Q^2)^2} \quad (10)$$

$w$  and  $w_0$  are the excluded volume parameters at the state of

measurement and at gel preparation, respectively

$$w = (1 - 2\chi + \nu_2)\nu_2 N \quad (11)$$

$$w_0 = (1 - 2\chi_0 + \nu_2^0)\nu_2^0 N \quad (12)$$

$Q$  is the reduced scattering vector normalized by the monomer fluctuating radius,  $Q = aN^{1/2}q$ ,  $\chi$  is the polymer–solvent interaction parameter, and the initial and final states of the gels are assumed to be in the mean field regime. Note that  $N$  is related to the effective crosslink density  $\nu_e$  through

$$N = 1/(\nu_e a^3 N_A) \quad (13)$$

where  $N_A$  is the Avogadro's number.

The solution of the above equations requires several parameters, which were evaluated as follows: We already know the crosslink density  $\nu_e$  (or  $N$ ) and the swelling capacity  $\nu_{2,\text{eq}}$  of gels as a function of  $\nu_2^0$  (Fig. 2 and Table 1). The interaction parameter  $\chi$  for PAAM–water system was recently evaluated using the Flory–Rehner equation as  $\chi = 0.481 \pm 0.005$  [23]. This value of  $\chi$  is independent on  $\nu_{2,\text{eq}}$  in the range of interest, that is,  $\chi = \chi_0$  [23]. The calculation of  $\chi$  assumes an equivalent size for both solvent (water) molecules and PAAM segments. Therefore, for the following calculations, the volume of segment ( $a^3$ ) was assumed to be equal to the molar volume of water (18 ml/mol), which

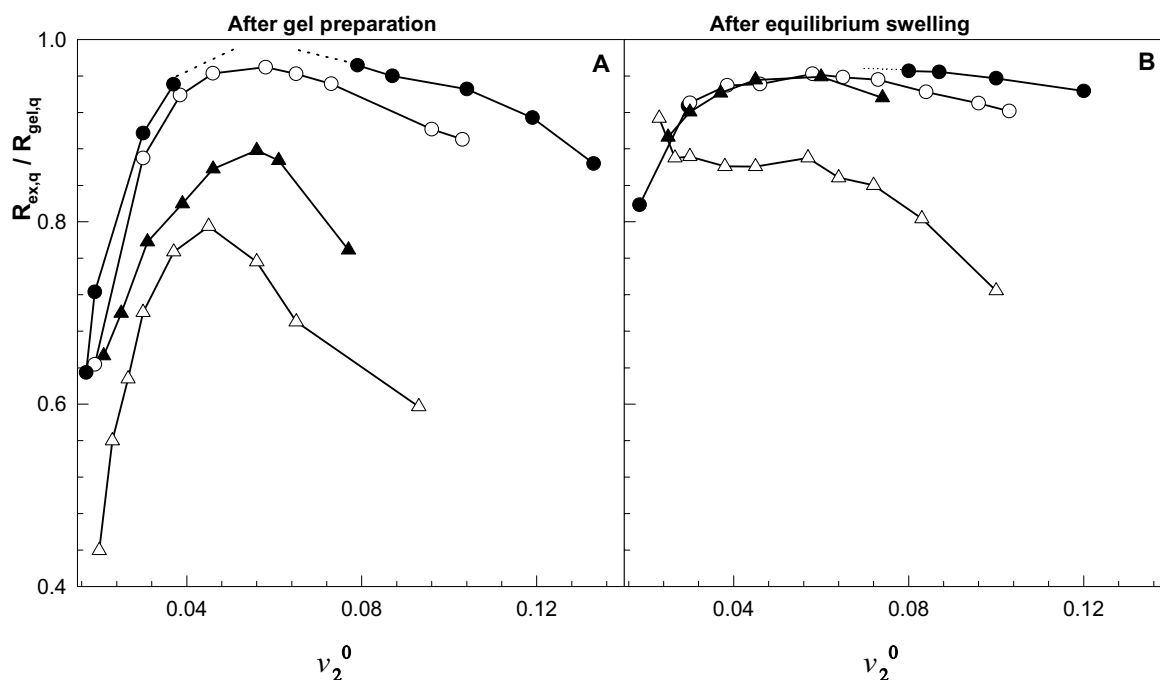


Fig. 5. The ratio  $R_{\text{ex},q}/R_{\text{gel},q}$ , representing the contribution of the spatial inhomogeneities to the scattering light intensity from PAAm gels is plotted against  $\nu_2^0$  for gels after preparation (A) and for the equilibrium swollen gels (B).  $X = 1/50$  (●),  $1/61.5$  (○),  $1/66$  (▲), and  $1/100$  (△). The curves show the trend of data.

leads to a segment length  $a = 3.1 \text{ \AA}$ . By substituting  $\nu_2 = \nu_2^0$  and  $\nu_2 = \nu_{2,\text{eq}}$  in Eqs. (7)–(13) for gels at the state of preparation and at the swollen state, respectively, the structure factor  $S(q)$ , its thermal fluctuations correlator  $G(q)$  and the part of static density inhomogeneities  $C(q)$  were calculated. Calculations were for the scattering vector  $q = 0.001 \text{ \AA}^{-1}$ .

In Fig. 7,  $S_q$  and  $G_q$  for PAAm gels after preparation (solid curves) and after equilibrium swelling in water (dashed curves) are shown as a function of  $\nu_2^0$ . Calculations were for the crosslinker ratio  $X = 1/66$ . Note that  $S_q$  and  $G_q$  are proportional to  $R_{\text{gel},q}$  and  $R_{\text{sol},q}$ , respectively. Comparison of the theoretical curves in Fig. 7 with the experimental data for the same set of gels given in Fig. 3 clearly shows that the theory correctly predicts the experimental behavior of gels. Structure factor for solutions does not change much while structure factor for gels significantly increases with the swelling of gels. A maximum in  $S_q$  is observed at both states of gels. In Fig. 8,  $C_q$  and the ratio  $C_q/S_q$ , which corresponds to the  $R_{\text{ex},q}/R_{\text{gel},q}$  data of gels, are shown as a function of  $\nu_2^0$  for each set of gels both after preparation (solid curves) and after equilibrium swelling (dotted curves). For comparison, the experimental  $R_{\text{ex},q}/R_{\text{gel},q}$  data for gels with  $X = 1/50$  and  $1/66$  are also shown in Fig. 8 by the symbols. In accord with the experiments, PR theory predicts an increase in the excess scattering  $C_q$  of gels during their swelling. This increase is significant for gels with the lower crosslinker ratios. Moreover, as found experimentally, swelling shifts  $\nu_{2,\text{cr}}^0$  toward smaller polymer concentrations. We should point out, however, that the agreement between the theory and the experiment is only in

qualitative nature. For example, as  $X$  is increased, the predicted  $\nu_{2,\text{cr}}^0$  for swollen gels slightly increases from 0.028 to 0.042, while the experimental  $\nu_{2,\text{cr}}^0$  increases from 0.030 to 0.06. Moreover, the contribution of excess scattering to the scattering intensity  $C_q/S_q$  is predicted to be 60 to 70% for swollen gels, which are smaller than those found by experiments (Fig. 8). These differences are probably due to the random crosslinking assumption of the PR theory, which is unrealistic for gels formed by free-radical mechanism [20,21].

In order to understand the physical origin of the experimental results, we consider three different effects playing an essential role in the apparent degree of the spatial gel inhomogeneities. These effects we will discuss are: crosslinker, concentration, and swelling effects. (1) Crosslinker effect: as seen in Fig. 1B, increase in  $\nu_2^0$  also increases the effective crosslink density  $\nu_e$  of the hydrogels. Previous work shows that PAAm gel becomes more inhomogeneous with increasing crosslink density [10–14]. Thus, as  $\nu_2^0$  is increased, the spatial inhomogeneity becomes larger due to the crosslinker effect. (2) Concentration effect: assuming that the effective crosslink density  $\nu_e$  remains constant over the entire range of  $\nu_2^0$ , one may expect a continuous decrease of the gel inhomogeneity on rising  $\nu_2^0$ . Indeed, calculations using the PR theory for a fixed  $\nu_e$  but varying  $\nu_2^0$  predict continuous decrease of  $C_q$  with increasing  $\nu_2^0$ . This is due to the fact that, the highly crosslinked (dense) regions of gel approach each other as the polymer concentration is increased, which reduce the concentration fluctuations between the densely and loosely crosslinked regions. (3) Swelling effect: to understand this effect, we consider an inhomogeneous gel as consisting of highly crosslinked

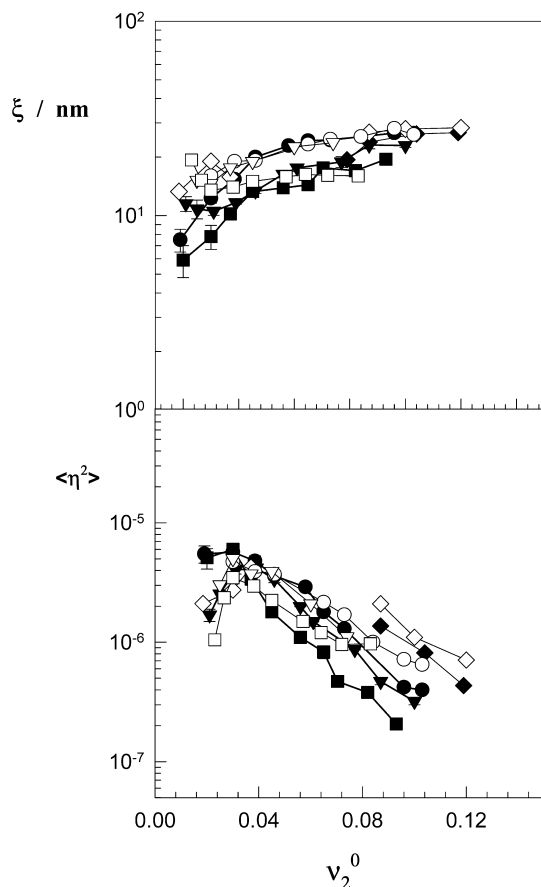


Fig. 6. The correlation length of the scatterers  $\xi$  and the mean square fluctuation of the refractive index  $\langle \eta^2 \rangle$  in PAAm gels shown as a function of  $\nu_2^0$ . The crosslinker ratio  $X$  of the hydrogels: 1/50 ( $\blacklozenge$ ), 1/61.5 ( $\bullet$ ), 1/66 ( $\blacktriangledown$ ), and 1/100 ( $\blacksquare$ ). Open symbols are for swollen gels while filled symbols are for gels after preparation.

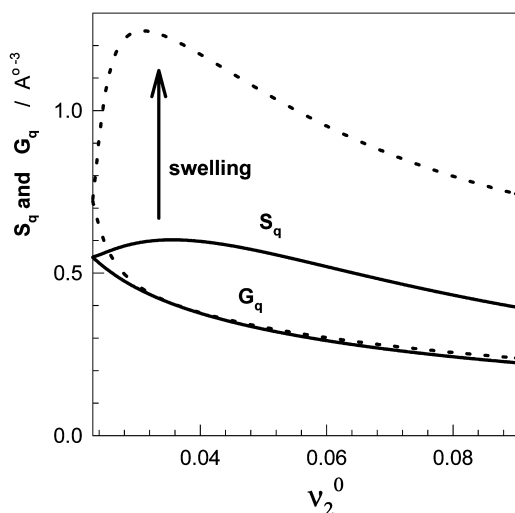


Fig. 7. Variation of the theoretical structure factor for gels ( $S_q$ ) and for solutions ( $G_q$ ) at  $q = 0.001 \text{ \AA}^{-1}$  with the polymer network concentration  $\nu_2^0$ . Calculations were using the PR theory and for PAAm gels with  $X = 1/66$  after preparation (solid curves) and after equilibrium swelling in water (dashed curves).

(dense) regions which are randomly distributed in a loosely crosslinked matrix polymer in the background. Since the crosslink density of the dense regions is larger than the average, these regions of gel partially shrink to ensure a micro-swelling equilibrium with the solvent in the environment. However, the matrix polymer is less crosslinked and therefore, the swelling capacity of this region is generally higher than the degree of dilution after the gel preparation. Thus, this region of gel is not in swelling equilibrium; if a good solvent is added, mainly the matrix polymer will swell further to attain the swelling equilibrium. As a consequence, concentration fluctuations and therefore, the spatial gel inhomogeneities will increase during the swelling process.

The  $\nu_2^0$  dependence of the gel inhomogeneity is thus determined by a competition of these effects. At low monomer concentrations, the first effect (crosslink density) is more dominant than the second effect (concentration) so that excess scattering increases with  $\nu_2^0$ . At higher values of  $\nu_2^0$ , the concentration effect dominates over the crosslink density effect, resulting in a continuous decrease in the excess scattering. The location of the maximum in the excess scattering vs. monomer concentration  $\nu_2^0$  plot represents the transition point between these two regimes. Moreover, decreasing the crosslinker ratio of gels also decreases the relative magnitude of the crosslinker effect (Fig. 1B), so that the concentration effect starts to dominate earlier, i.e. at a lower monomer concentration. Thus,  $\nu_{2,cr}^0$  shifts toward smaller concentration as the crosslinker ratio is decreased. Furthermore, if the gel swells beyond its swelling capacity after preparation, swelling effect starts to appear, which induces, opposing to the concentration effect, an increase in the excess scattering of gels. One may expect that the higher the swelling ratio, the larger the swelling capacity of the less crosslinked regions of gel, the larger the enhancement in the spatial inhomogeneity during gel swelling. In Fig. 9, the linear swelling ratio  $D/D_0$  of equilibrium swollen gels with respect to the after preparation state is plotted against  $\nu_2^0$ . It is seen that the gel samples from series  $X = 1/66$  and  $1/100$  swell much more than those from other series. The large increase of the spatial inhomogeneity upon swelling of these gels is thus associated with their high swelling capacities.

## 5. Conclusions

Results of experiments show the following scattering features of PAAm gels:

- (1) PAAm gels both at the state of preparation and at the equilibrium swollen state in water exhibit a maximum degree of spatial gel inhomogeneity at a critical monomer concentration  $\nu_{2,cr}^0$ .
- (2) Swelling enhances the extent of spatial gel inhomogeneities. This enhancement mainly occurs at low crosslinker ratios.

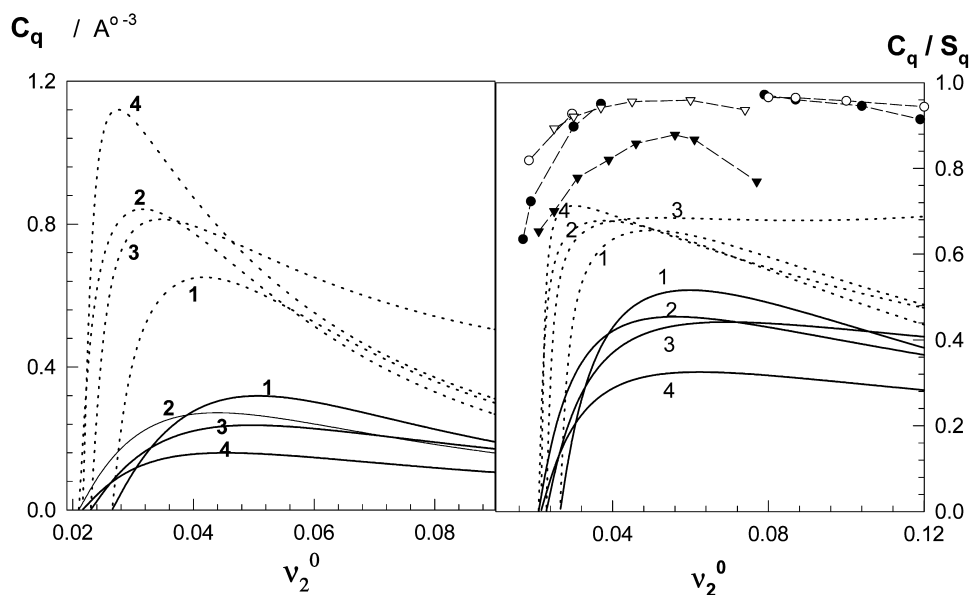


Fig. 8. Static density inhomogeneities  $C_q$  and the ratio  $C_q/S_q$  at  $q = 0.001 \text{ \AA}^{-1}$  shown as a function of  $v_2^0$ . Calculations were using the PR theory for PAAm gels after preparation (solid curves) and after equilibrium swelling in water (dotted curves). The crosslinker ratio  $X = 1/50$  (1),  $1/61.5$  (2),  $1/66$  (3),  $1/100$  (4). The experimental  $R_{ex,q}/R_{gel,q}$  data for gels with  $X = 1/50$  (●) and  $1/66$  (▼) are also shown for comparison. Filled symbols are for gels after preparation while open symbols for the equilibrium swollen gels. The dashed curves show the trend of the experimental data.

- (3)  $v_{2,cr}^0$  shifts toward smaller concentrations as the crosslinker ratio is decreased or, as the gel swells to its equilibrium swollen state.

The theoretical prediction of the PR theory was found to be in qualitative agreement with the experimental findings. It was also shown that three different effects, namely

crosslinker, concentration, and swelling effects determine the extent of inhomogeneities in gels formed at various monomer concentrations. The apparent degree of gel inhomogeneity is very sensitive to the relative magnitude of these effects. Therefore, monitoring the variation of excess scattering in gels depending on the monomer concentration is a good method for studying these effects.

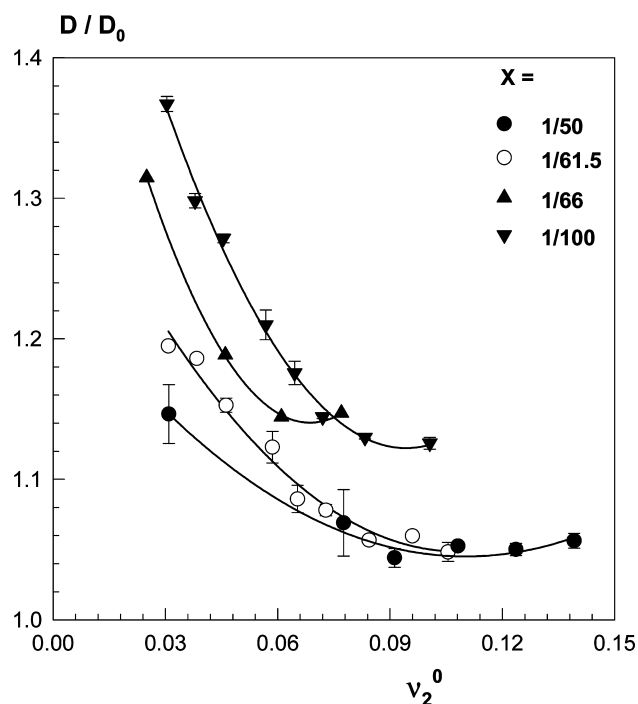


Fig. 9. Linear swelling ratio  $D/D_0$  of equilibrium swollen gels with respect to the after preparation state shown as a function of  $v_2^0$ . The crosslinker ratios of the hydrogels are indicated in the Figure.

## References

- [1] Shibayama M. *Macromol Chem Phys* 1998;199:1.
- [2] Bastide J, Candau SJ. In: Cohen Addad JP, editor. *Physical properties of polymeric gels*. New York: Wiley; 1996. p. 143.
- [3] Mallam S, Horkay F, Hecht AM, Geissler E. *Macromolecules* 1989; 22:3356.
- [4] Ikkai F, Shibayama M. *Phys Rev E* 1997;56:R51.
- [5] Cohen Y, Ramon O, Kopelman IJ, Mizraki S. *J Polym Sci Polym Phys Ed* 1992;30:1055.
- [6] Schosseler F, Skouri R, Munch JP, Candau SJ. *J Phys II* 1994;4:1221.
- [7] Shibayama M, Tanaka T, Han CC. *J Chem Phys* 1992;97:6842.
- [8] Horkay F, McKenna GB, Deschamps P, Geissler E. *Macromolecules* 2000;33:5215.
- [9] Lindemann B, Schröder UP, Oppermann W. *Macromolecules* 1997; 30:4073.
- [10] Shibayama M, Ikkai F, Nomura S. *Macromolecules* 1994;27:6383.
- [11] Shibayama M, Ikkai F, Shiwa Y, Rabin Y. *J Chem Phys* 1997;107: 5227.
- [12] Ikkai F, Iritani O, Shibayama M, Han CC. *Macromolecules* 1998;31: 8526.
- [13] Hecht AM, Duplessix R, Geissler E. *Macromolecules* 1985;18:2167.
- [14] Kizilay MY, Okay O. *Polymer* 2003;44:5239.
- [15] Moussaid A, Candau SJ, Joosten JGH. *Macromolecules* 1994;27: 2102.
- [16] Bueche F. *J Colloid Interf* 1970;33:61.
- [17] Geissler E, Horkay F, Hecht AM. *J Chem Phys* 1994;100:8418.

- [18] Mendes E, Lindner P, Buzier M, Boue F, Bastide J. *Phys Rev Lett* 1991;66:1595.
- [19] Bastide J, Mendes Jr E. *Makromol Chem Macromol Symp* 1990;40:81.
- [20] Funke W, Okay O, Joos-Muller B. *Adv Polym Sci* 1998;136:139.
- [21] Okay O. *Prog Polym Sci* 2000;25:711.
- [22] Baker JP, Hong LH, Blanch HW, Prausnitz JM. *Macromolecules* 1994;27:1449.
- [23] Kizilay MY, Okay O. *Macromolecules* 2003;36:6856.
- [24] Panyukov S, Rabin Y. *Macromolecules* 1996;29:7960.
- [25] Gundogan N, Melekaslan D, Okay O. *Macromolecules* 2002;35:5616.
- [26] Durmaz S, Okay O. *Polymer* 2000;41:3693.
- [27] Sayil C, Okay O. *Polymer* 2001;42:7639.
- [28] Flory PJ, *Principles of polymer chemistry*, Ithaca, NY: Cornell University Press; 1953.
- [29] Treloar LRG, *The physics of rubber elasticity*, Oxford: University Press; 1975.
- [30] Debye PJ. *J Chem Phys* 1959;31:680.
- [31] Debye P, Bueche AM. *J Appl Phys* 1949;20:518.
- [32] Soni VK, Stein RS. *Macromolecules* 1990;23:5257.
- [33] Horkay F, Hecht AM, Geissler E. *Macromolecules* 1994;27:1795.
- [34] Shibayama M, Tanaka T. *J Chem Phys* 1992;97:6829.
- [35] Wu W, Shibayama M, Roy S, Kurokawa H, Coyne LD, Nomura S, Stein RS. *Macromolecules* 1990;23:2245.
- [36] Higgins JS, Benoit HC, *Polymers and neutron scattering*, Oxford: Clarendon Press; 1994.
- [37] Baumgaertner A, Picot CE, *Molecular basis of polymer networks*, Berlin: Springer Verlag; 1989.